International Journal of Solids and Structures 51 (2014) 2336–2344

Contents lists available at ScienceDirect

International Journal of Solids and Structures

journal homepage: www.elsevier.com/locate/ijsolstr

Micromechanical study of elastic moduli of three-dimensional granular assemblies

N.P. Kruyt *

Department of Mechanical Engineering, University of Twente, P.O. Box 217, 7500 AE Enschede, The Netherlands

ARTICLE INFO

Article history:
Received 11 December 2013
Received in revised form 4 March 2014
Available online 31 March 2014

Keywords:
Granular materials
Elastic moduli
Micromechanics

ABSTRACT

In micromechanics of granular materials, relationships are investigated between micro-scale characteristics of particles and contacts and macro-scale continuum characteristics. For three-dimensional isotropic assemblies the macro-scale elastic characteristics are described by the bulk and the shear modulus, which depend on the micro-scale characteristics of the coordination number (i.e. the average number of contacts per particle) and the interparticle contact stiffnesses in directions normal and tangential to the contact.

It is well-known that the uniform-strain theory (or mean-field theory) overpredicts the elastic moduli. To find improved predictions, approximations of the particle displacement and rotations fields are obtained here by solving the equilibrium equations for small subassemblies that are centred around particles. At the boundary of these subassemblies, the particle displacements and rotations are prescribed such that they conform to the mean field.

Employing this approach, improved predictions of bulk and shear moduli are obtained, in comparison with those according to the uniform-strain assumption, especially when the size is increased of the subassemblies for which equilibrium equations are solved.

The elastic moduli are evaluated from the particle displacement and rotations fields by two methods. In the first, stress-based method the micromechanical expression for the average stress tensor, in terms of the forces at contacts and the branch vectors that connect particles in contacts, is employed. In the second, energy-based method the minimum potential-energy principle is used to obtain rigorous upper bounds to the moduli. It is generally observed that the moduli obtained from the stress-based method give closer agreement with the results from Discrete Element Method simulations than those from the energy-based method.

These improvements in the predictions of the elastic moduli are observed over the range of coordination numbers and interparticle stiffnesses considered here.

1. Introduction

Knowledge of the mechanical behaviour of granular materials is important in many industrial, geotechnical and geophysical applications dealing with granular materials. This knowledge is expressed as a constitutive relation, which can be formulated heuristically or from the micromechanical viewpoint. In the micromechanical approach a granular material is modelled as an assembly of particles that interact at contacts. This approach therefore incorporates the discrete nature of granular materials. An objective of micromechanics is to investigate relationships between micro-scale characteristics and macro-scale, continuum characteristics.

The objective of this study is to study, from the micromechanical viewpoint, the elastic properties of three-dimensional, isotropic granular assemblies. At the continuum, macro-scale these elastic properties are described by the elastic moduli that link (increments of) stress to (increments of) strain. At the micro-scale of contacts the interaction between particles is modelled by springs in directions normal and tangential to the contact. Some applications of the current model are the initial elastic deformation of granular materials and certain fibrous media. Elastic (and hence reversible) deformation of cohesionless granular materials is found for very small strains, typically for strains of 10^{-3}% for stress levels encountered in engineering applications (Tatsuoka, 1999) or in dynamic problems.

In contact mechanics (see for example Johnson, 1985) the interparticle interaction at the contact is often described by nonlinear

* Tel.: +31 53 489 2528; fax: +31 53 489 3695.
E-mail address: n.p.kruyt@utwente.nl

http://dx.doi.org/10.1016/j.ijsolstr.2014.03.002
0020-7683/

Hertz–Mindlin theory. The continuum elastic moduli are then dependent on the confining pressure, as studied theoretically (Digby, 1981; Walton, 1987; Goddard, 1990) and by Discrete Element Method (*DEM* for short) simulations (Makse et al., 2004; Agnolin and Roux, 2007a,b). In order to facilitate theoretical developments, here the interparticle stiffnesses are taken constant at all contacts. The values of the spring stiffnesses then depend on the confining pressure (as well as on the particle properties).

The elastic moduli of various regular packings of granular assemblies have been studied (Deresiewicz, 1958; Chang and Misra, 1989; Wang and Mora, 2009; Kruyt, 2012). Fleischmann et al. (2013a,b) used results for regular packings to obtain predictions of the Poisson ratio of fairly dense, disordered assemblies.

The uniform-strain assumption (or mean field assumption) has been frequently adopted in micromechanical studies of the elastic moduli of disordered systems (Rothenburg, 1980; Digby, 1981; Walton, 1987; Bathurst and Rothenburg, 1988a,b; Chang et al., 1990; Chang and Liao, 1994; Cambou et al., 1995). According to this assumption the relative displacement of two particles in contact is determined by the average displacement-gradient and the relative position vector of the particle centres. Corresponding predictions for the moduli are accurate for very dense assemblies, while for loose assemblies the moduli are significantly overpredicted (see for example Kruyt and Rothenburg, 1998, 2002, 2004; Makse et al., 1999; Rothenburg and Kruyt, 2001; Agnolin and Roux, 2007b; Magnanimo et al., 2008; Kruyt et al., 2010).

This limited adequacy of the uniform-strain assumption is due to the presence of *fluctuations* (relative to the deformation according to the uniform-strain assumption) that are induced by the geometrical disorder that is present in the assembly. DEM simulations have been used to study these fluctuations in two-dimensional assemblies (Kruyt and Rothenburg, 1998, 2002, 2004; Agnolin and Kruyt, 2008) and three-dimensional assemblies (Agnolin and Roux, 2008).

To find improved estimates of the elastic moduli for disordered systems, these fluctuations have been taken into account in theoretical studies that are completely analytical (Jenkins et al., 2005; Agnolin et al., 2006; La Ragione and Jenkins, 2007) or semi-numerical (Kruyt and Rothenburg, 2002, 2004; Agnolin and Kruyt, 2008; Agnolin and Roux, 2008; Kruyt et al., 2010). These theoretical approaches are based on considerations of the solutions of the equilibrium equations for small subassemblies. In the analytical, contact-based studies (Jenkins et al., 2005; Agnolin et al., 2006; La Ragione and Jenkins, 2007) the subassembly consists of a pair of particles in *contact* together with their neighbours. In the semi-numerical, particle-based studies (Kruyt and Rothenburg, 2002, 2004; Agnolin and Kruyt, 2008; Agnolin and Roux, 2008), the subassembly consists of a *particle* with its neighbours. In the analytical studies additional assumptions are employed to obtain approximate solutions to the equilibrium equations, while in the semi-numerical studies the equilibrium equations of the small subassemblies are solved numerically. These approaches are compared by Agnolin and Kruyt (2008) for the two-dimensional case and by Agnolin and Roux (2008) for the three-dimensional case. Generally, it is observed that the semi-numerical methods give more accurate predictions of the elastic moduli than the analytical methods.

Kruyt et al. (2010) extended the particle-based method to larger subassemblies for the two-dimensional case and found that this made it possible to obtain accurate predictions of the elastic moduli, even for loose assemblies with low coordination number (i.e. the average number of contacts per particle). The objective of this study is to extend this method to the three-dimensional case and to investigate its suitability for predicting the elastic moduli.

The outline of this study is as follows. Firstly, micromechanics of granular materials are summarised in Section 2. The uniform-strain assumption is described in Section 3, together with the corresponding elastic moduli. The proposed approach is detailed in Section 4. The employed isotropic assemblies and the Discrete Element Method simulations are characterised in Section 5. Results for the elastic moduli according to the various theories are presented in Section 6. Finally, findings of this study are discussed in Section 7.

2. Micromechanics

In this Section the basics of micromechanics of granular materials are described. Three-dimensional isotropic assemblies of spheres are considered. Small deformations are considered from an equilibrium configuration. Firstly, the contact geometry, statics and kinematics for the particles are described in Section 2.1. The elastic constitutive relation at the micro-scale, contact level is given in Section 2.2. The minimum potential-energy principle is summarised in Section 2.3. The uniform-strain assumption for predicting effective elastic moduli is described in Section 2.4.

2.1. Contact geometry, statics and kinematics

The interparticle contact areas are small, since the particles are stiff. The interparticle force is therefore considered as acting at the contact point. Contact moments, due to the distribution of traction over the contact region, are not considered here to keep the analysis simpler.

The vector from the centre of particle p to the contact point between particles p and q is denoted by $\boldsymbol{r}^{pq}$. The vector from the centre of particle p to the centre of particle q is denoted by $\boldsymbol{l}^{pq}$. This branch vector is given by

$$\boldsymbol{l}^{pq} = \boldsymbol{r}^{pq} - \boldsymbol{r}^{qp}. \tag{1}$$

For spherical particles where the deformation at contacts is small (i.e. the "overlap" of particles is small), we have

$$\boldsymbol{r}^{pq} = R^p \boldsymbol{n}^{pq} \text{ and } \boldsymbol{r}^{qp} = R^q \boldsymbol{n}^{qp}, \tag{2}$$

where R^p is the radius of particle p and $\boldsymbol{n}^{pq}$ is the (unit) contact normal vector directed from the centre of particle p to that of particle q. Note that $\boldsymbol{n}^{qp} = -\boldsymbol{n}^{pq}$.

The equilibrium equations for force and moment for particle p are given by

$$\sum_q \boldsymbol{f}^{pq} = \boldsymbol{0} \quad \sum_q \boldsymbol{r}^{pq} \times \boldsymbol{f}^{pq} = \boldsymbol{0}, \tag{3}$$

where $\boldsymbol{f}^{pq}$ is (the increment of) the interparticle force, exerted on particle p by particle q that is in contact with particle p, and the summation is over the particles q that are in contact with particle p.

The micromechanical expression for the average stress tensor $\boldsymbol{\sigma}$, in terms of the forces at contacts and the branch vectors, is given by (see for example Kruyt and Rothenburg, 1996)

$$\boldsymbol{\sigma} = \frac{1}{V} \sum_{c \in C} \boldsymbol{f}^c \boldsymbol{l}^c, \tag{4}$$

where the summation is over the contacts c in the set of contacts C and V is the volume (including voids) that is occupied by the assembly.

The particles have translational as well as rotational degrees of freedom. The displacement and rotation vectors of particle p are denoted by $\boldsymbol{u}^p$ and $\boldsymbol{\omega}^p$, respectively. The relative displacement vector $\boldsymbol{\Delta}^{pq}$ at the contact point between the particles p and q consists of contributions from particle displacements and rotations

$$\boldsymbol{\Delta}^{pq} = (\boldsymbol{u}^q + \boldsymbol{\omega}^q \times \boldsymbol{r}^{qp}) - (\boldsymbol{u}^p + \boldsymbol{\omega}^p \times \boldsymbol{r}^{pq}). \tag{5}$$

The contact constitutive relation gives the relation between (increments of) forces at contacts and (increments of) relative displacements. The elastic constitutive relation is considered in detail in the following subsection.

2.2. Elastic contact constitutive relation

The focus of the present paper is on elastic behaviour, which is appropriate for very small strains. For the description of the elastic behaviour at the contact level, the following assumptions are made: (1) contacts are cemented, i.e. the contact topology is fixed: contact creation and disruption are not taken into account and (2) interparticle Coulomb friction is ignored, since the number of interparticle contacts where Coulomb friction is fully mobilised ("sliding contacts") is small in the initial isotropic state. These assumptions make it possible to study truly *reversible* elastic behaviour, as Coulomb friction and the process of contact creation and disruption generally lead to irreversible behaviour (Calvetti et al., 2002).

The particle interaction at the contacts can be described by Hertz–Mindlin theory (see for example Johnson, 1985). This interaction is represented by nonlinear springs in directions normal and tangential to the contact, with contact stiffnesses k_n and k_t, respectively. In linearised analyses the values for these spring stiffnesses will in general depend on the equilibrium values for the normal forces, and hence on the value of the confining pressure.

The contact constitutive relation relating (the increment of) the force $\boldsymbol{f}^{pq}$ and (the increment of) the relative displacement $\boldsymbol{\Delta}^{pq}$ at the contact between particles p and q can now be expressed as

$$\boldsymbol{f}^{pq} = \boldsymbol{S}^{pq} \cdot \boldsymbol{\Delta}^{pq}, \tag{6}$$

where $\boldsymbol{S}^{pq}$ is the contact stiffness matrix that is determined by the contact spring stiffnesses k_n^{pq}, k_t^{pq} and the contact normal vector $\boldsymbol{n}^{pq}$

$$\boldsymbol{S}^{pq} = k_t^{pq}\boldsymbol{I} + (k_n^{pq} - k_t^{pq})\boldsymbol{n}^{pq}\boldsymbol{n}^{pq}, \tag{7}$$

where $\boldsymbol{I}$ is the three-dimensional identity matrix.

The equilibrium equations, Eq. (3), can be written concisely by defining the generalised force vector $\boldsymbol{F}^{pq}$ (of length 6) at the contact between particles p and q

$$\boldsymbol{F}^{pq} = \begin{bmatrix} \boldsymbol{f}^{pq} \\ \boldsymbol{n}^{pq} \times \boldsymbol{f}^{pq} \end{bmatrix}. \tag{8}$$

Note that, through the exclusion of the factor R^p in the moment term, all components of $\boldsymbol{F}^{pq}$ have the same dimension (or unit). The contact force satisfies Newton's third law, $\boldsymbol{f}^{qp} = -\boldsymbol{f}^{pq}$, but in general $\boldsymbol{F}^{qp} \neq -\boldsymbol{F}^{pq}$ for non-central forces ($\boldsymbol{n}^{pq} \times \boldsymbol{f}^{pq} \neq \boldsymbol{0}$).

In terms of the generalised forces $\boldsymbol{F}^{pq}$ the equilibrium equations, Eq. (3), become

$$\sum_q \boldsymbol{F}^{pq} = \boldsymbol{0}. \tag{9}$$

Analogously, the generalised displacement vector $\boldsymbol{U}^p$ (of length 6) is defined by

$$\boldsymbol{U}^p = \begin{bmatrix} \boldsymbol{u}^p \\ R^p\boldsymbol{\omega}^p \end{bmatrix}. \tag{10}$$

Note that, through the inclusion of the factor R^p in the rotation term, all components of $\boldsymbol{U}^p$ have the same dimension (or unit).

The generalised force $\boldsymbol{F}^{pq}$ is determined by the contact force $\boldsymbol{f}^{pq}$ through

$$\boldsymbol{F}^{pq} = \begin{bmatrix} \boldsymbol{I} \\ \boldsymbol{N}^{\times pq} \end{bmatrix} \cdot \boldsymbol{f}^{pq}, \tag{11}$$

where the operator $\boldsymbol{N}^\times = \boldsymbol{N}^\times(\boldsymbol{n})$ is defined such that $\boldsymbol{N}^\times \cdot \boldsymbol{v} = \boldsymbol{n} \times \boldsymbol{v}$ for all vectors $\boldsymbol{v}$. This means that $\boldsymbol{N}^\times$ is given by $\boldsymbol{N}^\times(\boldsymbol{n}) = -\boldsymbol{E} \cdot \boldsymbol{n}$ where $\boldsymbol{E}$ is the three-dimensional permutation symbol. Useful properties of the operator $\boldsymbol{N}^\times(\boldsymbol{n})$ are

$$\boldsymbol{N}^{\times T} = -\boldsymbol{N}^\times \quad \boldsymbol{N}^\times(-\boldsymbol{n}) = -\boldsymbol{N}^\times(\boldsymbol{n}). \tag{12}$$

The relation between the relative displacement $\boldsymbol{\Delta}^{pq}$ at the contact between particles p and q, Eq. (5), and their generalised displacements $\boldsymbol{U}^p$ and $\boldsymbol{U}^q$ can now be expressed compactly as

$$\boldsymbol{\Delta}^{pq} = [-\boldsymbol{I}\ \boldsymbol{N}^{\times pq}\boldsymbol{I}\ \boldsymbol{N}^{\times pq}] \cdot \begin{bmatrix} \boldsymbol{U}^p \\ \boldsymbol{U}^q \end{bmatrix} = \boldsymbol{B}^{pq} \cdot \begin{bmatrix} \boldsymbol{U}^p \\ \boldsymbol{U}^q \end{bmatrix}, \tag{13}$$

where the relation $\boldsymbol{N}^{\times qp} = -\boldsymbol{N}^{\times pq}$ (see Eq. (12)) has been used. Note that the first term in Eq. (13) inside the square brackets defines the matrix $\boldsymbol{B}^{pq}$ of size 3 by 12 that does not involve a subtraction.

The contact load at the contact between particles p and q, that combines the generalised forces $\boldsymbol{F}^{pq}$ and $\boldsymbol{F}^{qp}$, is now given in terms of the generalised displacements $\boldsymbol{U}^p$ and $\boldsymbol{U}^q$ by

$$\begin{bmatrix} \boldsymbol{F}^{pq} \\ \boldsymbol{F}^{qp} \end{bmatrix} = -(\boldsymbol{B}^{pq\,T} \cdot \boldsymbol{S}^{pq} \cdot \boldsymbol{B}^{pq}) \cdot \begin{bmatrix} \boldsymbol{U}^p \\ \boldsymbol{U}^q \end{bmatrix}, \tag{14}$$

as follows from Eqs. (11)–(13).

2.3. Minimum potential-energy principle

The minimum potential-energy principle is well-established in mechanics (see for example, Hill, 1950; Washizu, 1968). For granular materials an analogous discrete minimum potential-energy principle has been formulated by Kruyt and Rothenburg (2004) that incorporates the translational as well as the rotational degrees of freedom of the particles. Here this principle will be summarised, as it will be used subsequently to derive rigorous upper bounds to the elastic moduli.

At the boundary B of the assembly the displacements are prescribed. Two displacement and rotation fields $\{\boldsymbol{u}^p, \boldsymbol{\omega}^p\}$ and $\{\boldsymbol{u}^{*p}, \boldsymbol{\omega}^{*p}\}$ for the particles are considered, which both satisfy the displacement boundary conditions at B. These displacement and rotation fields have associated relative displacement fields $\{\Delta^c\}$ and $\{\Delta^{*c}\}$, according to Eq. (5). The corresponding contact force fields $\{\boldsymbol{f}^c\}$ and $\{\boldsymbol{f}^{*c}\}$ are determined from the contact constitutive relation Eq. (6). By definition, the contact force field $\{\boldsymbol{f}^c\}$ satisfies all equilibrium conditions Eq. (3), contrary to the contact force field $\{\boldsymbol{f}^{*c}\}$.

The discrete minimum potential-energy principle then reads

$$\begin{aligned} \prod(\{\boldsymbol{u}^p, \boldsymbol{\omega}^p\}) &\equiv \frac{1}{2V}\sum_{c\in C} \boldsymbol{f}^c \cdot \boldsymbol{\Delta}^c \leqslant \frac{1}{2V}\sum_{c\in C} \boldsymbol{f}^{*c} \cdot \boldsymbol{\Delta}^{*c} \\ &\equiv \prod(\{\boldsymbol{u}^{*p}, \boldsymbol{\omega}^{*p}\}). \end{aligned} \tag{15}$$

This energy principle states that the true displacement and rotation fields $\{\boldsymbol{u}^p, \boldsymbol{\omega}^p\}$, whose contact force field $\{\boldsymbol{f}^c\}$ satisfies the equilibrium conditions Eq. (3), make the potential-energy density Π an absolute minimum among all displacement and rotation fields $\{\boldsymbol{u}^{*p}, \boldsymbol{\omega}^{*p}\}$ that satisfy the boundary conditions.

2.4. Uniform strain and fluctuations

According the uniform-strain assumption (or mean-field assumption), the displacements of all particles are determined by the mean displacement gradient $\boldsymbol{\alpha}$, with components $\alpha_{ij} = \partial u_i / \partial x_j$. The particle rotations are all identical to the average rotation vector $\boldsymbol{\Omega}$. Hence

$$\boldsymbol{u}^p = \boldsymbol{\alpha} \cdot \boldsymbol{X}^p \quad \boldsymbol{\omega}^p = \boldsymbol{\Omega}. \tag{16}$$

In classical continuum mechanics the components Ω_i of the average rotation vector are determined from the displacement gradient (see for example Aris, 1962)

$$\Omega_i = -\frac{1}{2} E_{ijk}\alpha_{jk}, \tag{17}$$

where E_{ijkl} are the components of the three-dimensional permutation symbol.

It follows from Eqs. (5), (16), and (17) that the relative displacement according to the uniform-strain assumption, $\bar{\Delta}^{pq}$, is given by

$$\bar{\Delta}^{pq} = \boldsymbol{\varepsilon}\cdot\boldsymbol{l}^{pq}, \tag{18}$$

where $\boldsymbol{\varepsilon}$ is the (symmetrical) strain tensor in classical continuum mechanics

$$\boldsymbol{\varepsilon} = \frac{1}{2}(\boldsymbol{\alpha} + \boldsymbol{\alpha}^T). \tag{19}$$

The actual displacement and rotation of a particle can be expressed as the sum of those according to the uniform-strain assumption and a *fluctuation*. This means that the displacement fluctuation $\boldsymbol{u}'^p$ is defined as the difference between the actual displacement $\boldsymbol{u}^p$ and that according to the uniform-strain assumption. An analogous decomposition is employed for the particle rotation, where $\boldsymbol{\omega}'^p$ is the fluctuation in rotation of particle p. Hence

$$\begin{aligned}\boldsymbol{u}^p &= \boldsymbol{\alpha}\cdot\boldsymbol{X}^p + \boldsymbol{u}'^p\\ \boldsymbol{\omega}^p &= \boldsymbol{\Omega} + \boldsymbol{\omega}'^p.\end{aligned} \tag{20}$$

This definition of the fluctuations effectively represents a change of variable, from particle displacements $\boldsymbol{u}^p$ and rotations $\boldsymbol{\omega}^p$ to the corresponding fluctuations, $\boldsymbol{u}'^p$ and $\boldsymbol{\omega}'^p$. These fluctuations are expected to be spatially homogeneous (in a statistical sense), contrary to the particle displacements $\boldsymbol{u}^p$ and rotations $\boldsymbol{\omega}^p$, due to the presence of the position-dependent mean-field contribution.

The generalised displacement $\boldsymbol{U}^p$ of particle p is decomposed accordingly into a uniform-strain contribution $\bar{\boldsymbol{U}}^p$ and a fluctuation $\boldsymbol{U}'^p$

$$\boldsymbol{U}^p = \bar{\boldsymbol{U}}^p + \boldsymbol{U}'^p \tag{21}$$

In terms of the fluctuations in the generalised displacements, $\boldsymbol{U}'^p$, the generalised equilibrium equations Eq. (9) for particle p become

$$\sum_q \begin{bmatrix}\boldsymbol{I}\\ \boldsymbol{N}^{\times pq}\end{bmatrix}\cdot\boldsymbol{S}^{pq}\cdot\boldsymbol{B}^{pq}\cdot\begin{bmatrix}\boldsymbol{U}'^p\\ \boldsymbol{U}'^q\end{bmatrix} = -\sum_q \begin{bmatrix}\boldsymbol{I}\\ \boldsymbol{N}^{\times pq}\end{bmatrix}\cdot\boldsymbol{S}^{pq}\cdot\bar{\boldsymbol{\Delta}}^{pq}, \tag{22}$$

where Eqs. (6), (11), (13), and (18) have been employed. Note that these linear equations for the fluctuations in the generalised displacements, $\boldsymbol{U}'^p$, are coupled.

3. Elastic moduli according to uniform-strain assumption

For linear elastic behaviour the macro-scale continuum stress (increments) $\boldsymbol{\sigma}$ and strain (increments) $\boldsymbol{\varepsilon}$ are related by the (constant) fourth-order elastic stiffness tensor $\boldsymbol{L}$

$$\boldsymbol{\sigma} = \boldsymbol{L} : \boldsymbol{\varepsilon}. \tag{23}$$

For isotropic materials its components L_{ijkl} can be expressed as

$$L_{ijkl} = \lambda\delta_{ij}\delta_{kl} + 2\mu\delta_{ik}\delta_{jl}, \tag{24}$$

where δ_{ij} is the Kronecker symbol and the Lamé constants λ and μ are related to the bulk and shear moduli K and G by

$$K = \lambda + \frac{2}{3}\mu \quad G = \mu. \tag{25}$$

In terms of the bulk and the shear moduli K and G, the relation between stress and strain is given by

$$\boldsymbol{\sigma} = \left(K - \frac{2}{3}G\right)(tr\boldsymbol{\varepsilon})\boldsymbol{I} + 2G\boldsymbol{\varepsilon} = K(tr\boldsymbol{\varepsilon})\boldsymbol{I} + 2G\mathrm{dev}\boldsymbol{\varepsilon}, \tag{26}$$

where $\mathrm{dev}\boldsymbol{\varepsilon} = \boldsymbol{\varepsilon} - 1/3(\mathrm{tr}\boldsymbol{\varepsilon})\boldsymbol{I}$ is the deviator of $\boldsymbol{\varepsilon}$.

Here the arguments leading to expressions for the elastic moduli according to the uniform-strain assumption are summarised (see also Bathurst and Rothenburg, 1988a; Chantawarangul, 1993). According to the uniform-strain assumption the relative displacements at contacts are given by Eq. (18). The corresponding contact forces follow from Eq. (6), with spring stiffnesses k_n and k_t in Eq. (7) that are taken identical at all contacts. Then the stress tensor $\boldsymbol{\sigma}$ is evaluated from the micromechanical expression for the stress tensor, Eq. (4)

$$\boldsymbol{\sigma} = m_V\int_n E(\boldsymbol{n})[\boldsymbol{S}(\boldsymbol{n})\cdot\boldsymbol{\varepsilon}\cdot l(\boldsymbol{n}))]\boldsymbol{l}(\boldsymbol{n})d\Omega(\boldsymbol{n}). \tag{27}$$

The equality follows from Eq. (4) by grouping contacts by orientation and by the transition to a continuous probability distribution of contact orientations that are determined by the contact normal $\boldsymbol{n}$. Here $m_V = N_c/V$ is the contact density (with N_c the number of contacts), $E(\boldsymbol{n})$ is the contact distribution function (Horne, 1965) and $d\Omega$ is the solid-angle element, $d\Omega = \sin\theta d\theta d\phi$ where θ and ϕ are the azimuthal and circumferential angles, respectively, in spherical coordinates that describe the orientation of the contact normal vector $\boldsymbol{n}$. For the isotropic assemblies that are considered here, $E(\boldsymbol{n}) = 1/(4\pi)$. The branch vector $\boldsymbol{l}(\boldsymbol{n}) \cong 2\bar{R}\boldsymbol{n}$ for assemblies which are approximately monodisperse, where $\bar{R}$ denotes the average of the particle radius.

Since the solid fraction φ is determined by the number of particles N_p and the average volume per particle $\frac{4}{3}\pi\overline{R^3}$, it follows that the solid fraction is given by $\varphi = \left(N_p\frac{4}{3}\pi\overline{R^3}\right)/V)$. Coordination number Z (i.e. the average number of contacts per particle) is determined by the number of contacts N_c and the number of particles N_p: $Z = (2N_c)/N_p$ (the factor 2 is present since each interparticle contact is 'shared' between two particles). It follows that the contact density m_v is related to the solid fraction φ, coordination number Z and characteristics of the particle-size distribution by

$$m_V = \frac{3}{8\pi}\frac{\varphi Z}{\bar{R^3}}. \tag{28}$$

The resulting bulk and shear modulus according to the uniform-strain assumption, K^ε and G^ε respectively, are given in dimensionless form by (see also Chantawarangul, 1993)

$$\frac{K^\varepsilon\bar{R}}{k_n} = \frac{1}{6\pi}\left(\frac{\overline{R^2}\bar{R}}{\overline{R^3}}\right)\varphi Z \qquad \frac{G^\varepsilon\bar{R}}{k_n} = \frac{1}{10\pi}\left(\frac{\overline{R^2}\bar{R}}{\overline{R^3}}\right)\varphi Z\left(1 + \frac{3}{2}\frac{k_t}{k_n}\right). \tag{29}$$

4. Local-adjustment-field approach

The approach of the "local adjustment field" (Kruyt and Rothenburg, 2002, 2004; Kruyt et al., 2010) forms an approximation of the actual problem of determining the particle displacements and rotations such that equilibrium is attained for the complete assembly. In the simplest form of the local-adjustment-field approach, the generalised displacement of a particle p is determined by assuming that its neighbours, with which it is in contact, move according to the uniform-strain assumption Eq. (16). The fluctuations in generalised displacement $\{\boldsymbol{U}'^q\}$ of these neighbours q then are zero in Eq. (22). The generalised fluctuation displacement vector $\{\boldsymbol{U}'^p\}$ of particle p can then be determined from the generalised equilibrium equations, Eq. (22). This process can be repeated for all particles in the assembly. This yields a field (or set) of generalised displacements $\{\boldsymbol{U}'^p\}$, based on *local adjustments* (relative to the uniform-strain displacement field) in order to satisfy the equilibrium equations. This approach has been proposed by Kruyt and Rothenburg (2002) for the two-dimensional case where particle rotations were suppressed and by Kruyt and Rothenburg (2004) for the two-

dimensional case with particle rotations and by Agnolin and Roux (2008) for the three-dimensional case with particle rotations.

The described approach, in which the equilibrium equations are solved for a small subassembly, or *shell*, consisting of a single particle (that has free displacements and rotations) with its neighbours (that have prescribed displacements and rotations), has been generalised to larger shells by Kruyt et al. (2010) for the two-dimensional case. At the next size of the shell, m, for a certain central particle (that has free displacements and rotations), its neighbours are assumed also to have free displacements and rotations. Their neighbours (excluding the central particle) have prescribed displacements and rotations according to the average displacement-gradient. These shells are illustrated in Fig. 1 for different sizes m, or orders, of the shells. The displacements and rotations of the inner particles of the shell are determined by solving the equilibrium equations for such small subassemblies. From this solution, only the displacement and rotation vectors of the central particle are retained.

This idea can be expressed more formally. The particles and the interparticle contacts form a graph, where the particles correspond to vertices and the contacts correspond to edges. The graph-distance between two particles is the number of edges in a shortest path between these particles. For an order of the shell m, those particles are in the shell that have a graph-distance to the central particle that is equal to or smaller than m. The outer particles of the shell have a graph-distance that is equal to m, the order of the shell.

The equilibrium equations for the subassembly that corresponds to the shell, of order m, can be formulated in the way as described in detail by Kruyt et al. (2010) for the two-dimensional case. The shell represents a structure, where kinematic boundary conditions apply at the outer particles of the shell. These kinematic boundary conditions are according to Eq. (14). The connectivity of the structure is determined by the interparticle contacts. The interaction between the particles is described by Eq. (14), which gives the "element matrix" in Finite Element Method terminology.

The process of finding the particles in the shell corresponding to a central particle, constructing and solving the linear system of equilibrium equations is repeated for all particles. For each central particle, only the generalised displacement fluctuation is retained for the generalised displacement field. This gives an approximate field of fluctuations in particle displacements and rotations $\{\boldsymbol{u}^{*p}, \boldsymbol{\omega}^{*p}\}$, which is used to estimate the elastic moduli as explained in the following subsection.

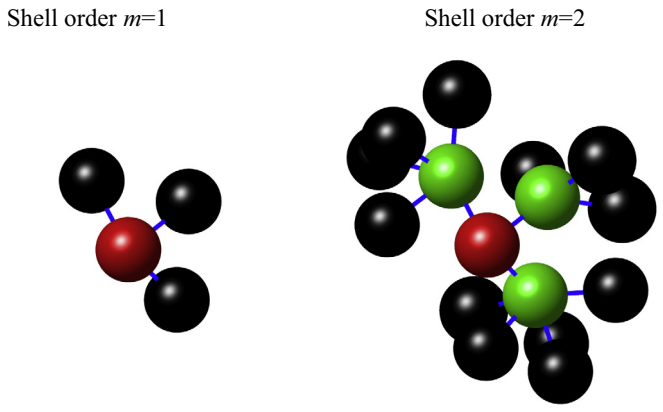

Fig. 1. Illustration of shells. These shells are constructed around a central particle that is shown in red. The outer particles of the shells are shown in black. The displacements and rotations of these outer particles are according to the uniform-strain assumption. Left: order of shell $m = 1$. The central particle with its neighbours, that are in contact with the central particle, are shown. Right: order of shell $m = 2$. The central particle and its neighbours (shown in green) are shown, together with their neighbours. Interparticle contacts are indicated by blue lines that connect the particle centres. The radii of the particles have been reduced (i.e. the particles have been shrunk) to facilitate the viewing of these interparticle contacts. (For interpretation of the references to color in this figure legend, the reader is referred to the web version of this article.)

It is emphasised that the local-adjustment-field approach is an approximation, as the particle displacement and rotation fields are determined from solutions of equilibrium equations for *sub*assemblies instead of for the complete assembly. Consequently, the contact forces associated with the estimated displacement and rotation fields will not exactly satisfy the equilibrium equations for the particles, but deviations from equilibrium are expected to become smaller as the shell size m is increased.

In the local-adjustment-field approach displacements that are prescribed at the boundary are not affected, as the fluctuations are equal to zero at the boundary. Since the average displacement gradient is determined by the displacement distribution at the boundary, the local-adjustment-field approach is always consistent with the prescribed average displacement-gradient.

4.1. Estimation of moduli

Estimates of elastic moduli can be obtained in two different ways from the local adjustment fields $\{\boldsymbol{u}^{*p}, \boldsymbol{\omega}^{*p}\}$, as described by Kruyt et al. (2010).

In the *stress-based* evaluation of the moduli, contact forces $\boldsymbol{f}^{*c}$ that correspond to $\{\boldsymbol{u}^{*p}, \boldsymbol{\omega}^{*p}\}$ are determined from the contact constitutive relation, Eq. (6). Note that the force $\boldsymbol{f}^{*pq}$ at the contact between particles p and q involves the fluctuations of particles p and q (see also Eq. (5)). Using the micromechanical expression for the stress tensor, Eq. (4), a stress tensor is obtained. This yields an estimate of the elastic modulus corresponding to the loading path under consideration with a prescribed displacement gradient.

Alternatively, in the *energy-based* evaluation of the moduli, the generalised displacement field is employed to obtain an estimate of the energy present in the springs, i.e. the potential-energy density $\Pi(\{\boldsymbol{u}^{*p}, \boldsymbol{\omega}^{*p}\})$ in Eq. (15) is evaluated. Since $(1/2)\varepsilon_{ij}L_{ijkl}\varepsilon_{kl} = \Pi(\{\boldsymbol{u}^{p}, \boldsymbol{\omega}^{p}\}) \leqslant \Pi(\{\boldsymbol{u}^{*p}, \boldsymbol{\omega}^{*p}\})$, with $\{\boldsymbol{u}^{p}, \boldsymbol{\omega}^{p}\}$ the true solution to all equilibrium equations, a rigorous *upper bound* (and hence an estimate) to the elastic moduli is obtained.

For the true displacement and rotation field $\{\boldsymbol{u}^{p}, \boldsymbol{\omega}^{p}\}$, the energy-based and the stress-based approaches yield the same value for the elastic modulus.

4.2. Computational complexity of local-adjustment-field approach

Here the computational complexity of local-adjustment-field approach is analysed. This analysis provides an order of magnitude estimate of the number of computer operations required for the solution of the equilibrium equations for the shells. To keep the analysis simple, it is based on considerations of direct solution methods for linear systems of equations that involve full matrices (rather than more efficient methods that are based on direct solution techniques involving sparse matrices or on iterative methods; see for example Golub and van Loan, 1996). For a full matrix, this operation count OC scales with the size of the matrix N as $OC \sim N^3$. The number of operations for the solution of the equilibrium equations for the full assembly then scales as $OC_{\text{full}} \sim N_p^3$. For a shell of order m, the number of particles inside the shell, N_s, scales as m^3. The number of operations OC_{shell} for the solution of N_p shell equilibrium equations then scales as $OC_{\text{shell}} \sim N_p m^9$. This means that the required computing time of local-adjustment-field approach increases very rapidly with increasing shell order m.

5. Assemblies and DEM simulations

Four isotropic assemblies have been generated through DEM simulations (Cundall and Strack, 1979) of isotropic compression to a specified pressure p. During the compression phase interparticle friction is present and contacts may be created or disrupted (i.e. contacts are not fixed). For these assemblies the nondimensional ratio $(p\bar{R})/k_n$ equals 0.9×10^{-3}, 3×10^{-3}, 7×10^{-3} and 14×10^{-3}, with $\bar{R}$ the average particle radius. These assemblies consist of 30,000 bidisperse spheres (radii $R_1/\bar{R}=1.025$ and $R_2/\bar{R}=0.975$ with equal numbers of spheres with radii R_1 and R_2). Periodic boundary conditions have been employed to eliminate wall effects. The size of the cubic periodic box is approximately 30 particle diameters for the densest assembly.

The dependence of the coordination number Z on the confining pressure p for these assemblies is shown in Fig. 2 (left). In the determination of the coordination number Z, unstable particles (so-called rattlers) with fewer than three contacts are not taken into account, as they do not affect the mechanical properties of the system. Since friction is included in the compression phase, loose assemblies with coordination number Z below 6, the isostatic value for frictionless assemblies, are obtained.

The relation between the coordination number Z and the solid fraction φ for the employed assemblies is shown in Fig. 2(right). For each assembly two values for the solid fraction φ have been calculated. For the first, higher value the volume occupied by the rattlers is taken into account in the calculation of the total particle volume, while for the second value this volume is not taken into account.

The results shown in Fig. 2 indicate that an increase in pressure p is associated with a denser packing, i.e. an increase in coordination number Z and in solid fraction φ. Note that there is no unique relation between coordination number and solid fraction and pressure for frictional assemblies (see for example Agnolin and Roux (2007a)).

To obtain values of the true elastic moduli, DEM simulations have been performed in accordance to the assumptions discussed in Section 2.2, with fixed contacts (i.e. without contact creation and disruption) and without Coulomb frictional limit (corresponding to an infinite interparticle friction coefficient). Spring constants k_n and k_t have been taken identical at all contacts.

Loading paths that have been considered are

$$\boldsymbol{\varepsilon}^K=\varepsilon_0\begin{bmatrix}1&0&0\\0&1&0\\0&0&1\end{bmatrix}\text{ and }\boldsymbol{\varepsilon}^G=\varepsilon_0\begin{bmatrix}1&0&0\\0&-\frac{1}{2}&0\\0&0&-\frac{1}{2}\end{bmatrix},\tag{30}$$

where $\varepsilon_0=10^{-3}$ is a magnitude of the imposed strain increment. The first and second loading paths are used to determine the bulk modulus K and the shear modulus G, respectively.

6. Results

Here the predictions for the moduli according to the local-adjustment-field approach and the uniform-strain assumption are compared to the true moduli from the DEM simulations. Both the bulk modulus K and the shear modulus G are considered. For these cases the loading conditions correspond to the strain tensors given by Eq. (30).

Since rattlers do not contribute to the stress, they are not considered in the local-adjustment-field approach.

The influence of the shell size on the predictions of the moduli is investigated in Section 6.1, while the influence of the coordination number Z of the assembly and the stiffness ratio k_t/k_n that characterises the particle interaction are studied in Sections 6.2 and 6.3, respectively.

6.1. Effect of shell size

The influence of the shell size m on the predictions of the bulk modulus K and shear moduli G is shown in Fig. 3, left and right, respectively, for the fairly dense assembly with coordination number $Z=5.52$ and for a stiffness ratio $k_t/k_n=0.8$. The stress-based and the energy-based predictions (see Section 4.1) are both shown, as well as the predictions according to the uniform-strain assumption (see Eq. (29)) and the true moduli determined from the results of the DEM simulations.

For both bulk modulus K and shear modulus G, the local-adjustment-field predictions get closer to the true elastic moduli from the DEM simulations for increasing shell order m. Thus, more accurate descriptions of the particle displacement and rotation fields have been obtained when these are found by determining these from the equilibrium equations involving shells of increasing size m.

The energy-based prediction is always larger than the true DEM value, since the energy-based prediction forms a rigorous upper

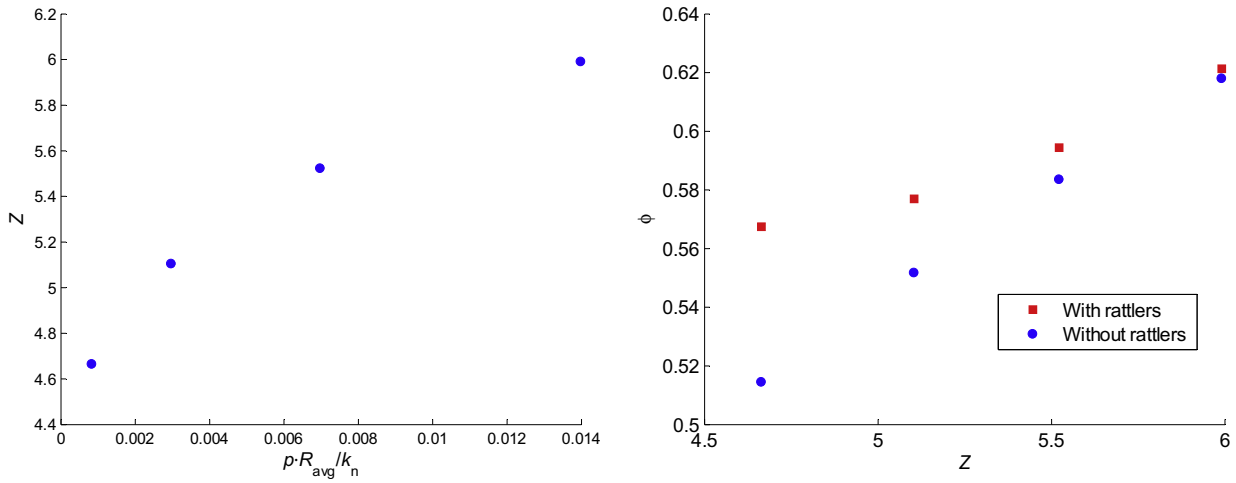

Fig. 2. Characteristics of employed isotropic assemblies. Left: coordination number Z as a function of imposed pressure p. Right: solid fraction φ as a function of coordination number Z.

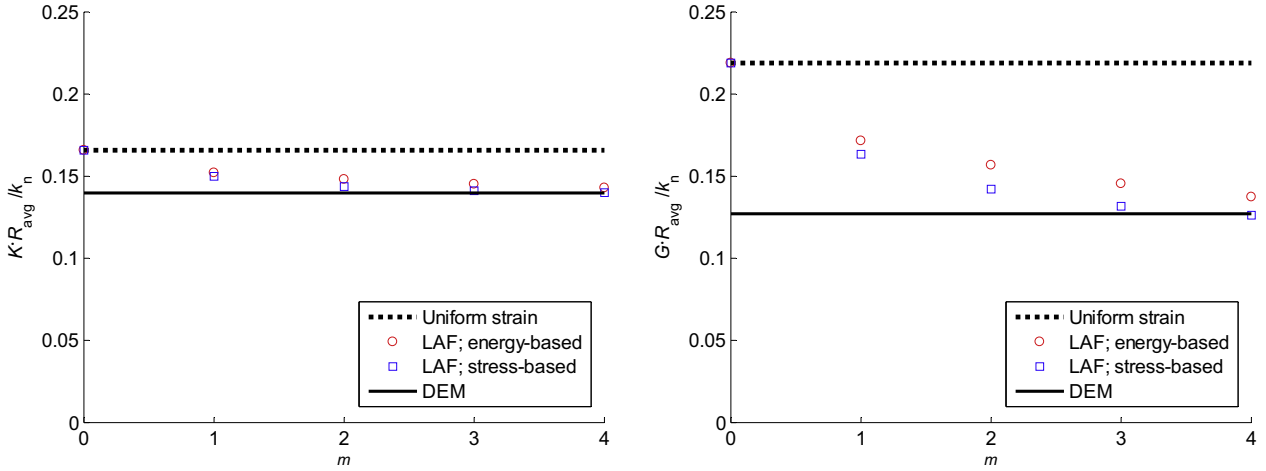

Fig. 3. Influence of shell size m on predicted elastic moduli using the local-adjustment-field (LAF) approach. Also shown are the predictions according to the uniform-strain assumption and the true moduli from the DEM simulations. Left: bulk modulus K; right: shear modulus G. Assembly with coordination number $Z = 5.52$ and stiffness ratio $k_t/k_n = 0.8$.

bound, as explained in Section 2.3. In contrast, the stress-based prediction may fall slightly below the DEM value (see Fig. 3, right for $m = 4$). The difference between stress-based and energy-based estimates is smaller for the bulk modulus K than for the shear modulus G.

For the shell size $m = 3$, the relative deviation between true DEM bulk modulus K and stress-based and energy-based predictions is 1% and 4%, respectively. The corresponding relative deviations for the shear modulus G are 4% and 14% for the stress-based and the energy-based predictions, respectively.

The stress-based estimate forms an upper bound (see Section 4.1), while for the stress-based estimate differences in the corresponding forces, in comparison with the true force field, may cancel out to some degree. These considerations make it plausible that the stress-based estimate is generally closer to the true modulus than the corresponding energy-based estimate. Note again that for the true displacement and rotation field, both estimates yield the same result (see Section 4.1).

Since the stress-based predictions of the moduli are closer to the true modulus from the DEM simulations than the energy-based predictions, the stress-based predictions will be used for the results shown in the following subsections.

6.2. Effect of coordination number

The results shown in the previous subsection have demonstrated that the local-adjustment-field approach works well for a fairly dense assembly. Here it is investigated how the local-adjustment-field approach works for assemblies with other coordination numbers Z (in particular for looser assemblies with lower coordination numbers), but with the same value of the stiffness ratio $k_t/k_n = 0.8$.

The results are shown in Fig. 4 for the bulk modulus K and the shear modulus G on the left and right, respectively. For all coordination numbers Z considered, the results show that local-adjustment-field predictions of the elastic moduli get closer to the true value from the DEM simulations with increasing shell size m.

For the shell size $m = 3$, the relative deviations between true, DEM moduli and predictions vary from 1% to 6% for the bulk modulus and from 2% to 16% for the shear modulus. More accurate predictions are observed for denser assemblies with higher coordination numbers Z. For lower coordination number Z, the particles are less constrained, resulting in larger fluctuations in particle displacements and rotations. These larger fluctuations are only partly captured by the local-adjustment-field approach, leading to less accurate predictions of the elastic moduli at lower coordination number Z.

6.3. Effect of stiffness ratio

Here it is investigated how the local-adjustment-field approach works for different values of the stiffness ratio k_t/k_n (in the range 0.2–1.0) that characterises the particle interaction, for the assembly with coordination number $Z = 5.52$.

The results are shown in Fig. 5. The DEM results show that the bulk modulus K shows a weak dependence on the stiffness ratio k_t/k_n, while the uniform-strain theory predicts (incorrectly) that the bulk modulus is independent of the stiffness ratio, see Eq. (29). The local-adjustment-field approach captures this weak dependence of the bulk modulus K on the stiffness ratio k_t/k_n. This was also noted by Kruyt et al. (2010) for two-dimensional assemblies. The difference between true DEM shear modulus and that according to the uniform-strain assumption is quite significant.

For the shell size $m = 3$, the relative deviations between true, DEM moduli and predictions vary from 1% to 2% for the bulk modulus and from 3% to 6% for the shear modulus. Slightly more accurate predictions are obtained for lower values of the stiffness ratio. For lower stiffness ratio k_t/k_n, the coupling of the particles through the rotational degrees of freedom becomes weaker, and the fluctuations in particle displacements and rotations are smaller. These smaller fluctuations are therefore better captured by the local-adjustment-field approach, leading to (slightly) more accurate predictions of the elastic moduli at lower stiffness ratio k_t/k_n for this fairly dense assembly.

6.4. Comparison of two-dimensional and three-dimensional cases

The current three-dimensional method is an extension of the two-dimensional method of Kruyt et al. (2010). A difference between these cases is in the number of translational and rotational degrees of freedom per particle. In the two-dimensional case, there are two translational and one rotational degrees of freedom per particle. In the three-dimensional case, there are three translational and three rotational degrees of freedom per particle. Thus, the importance of rotational degrees of freedom is expected to be larger in the three-dimensional case than in the two-dimensional

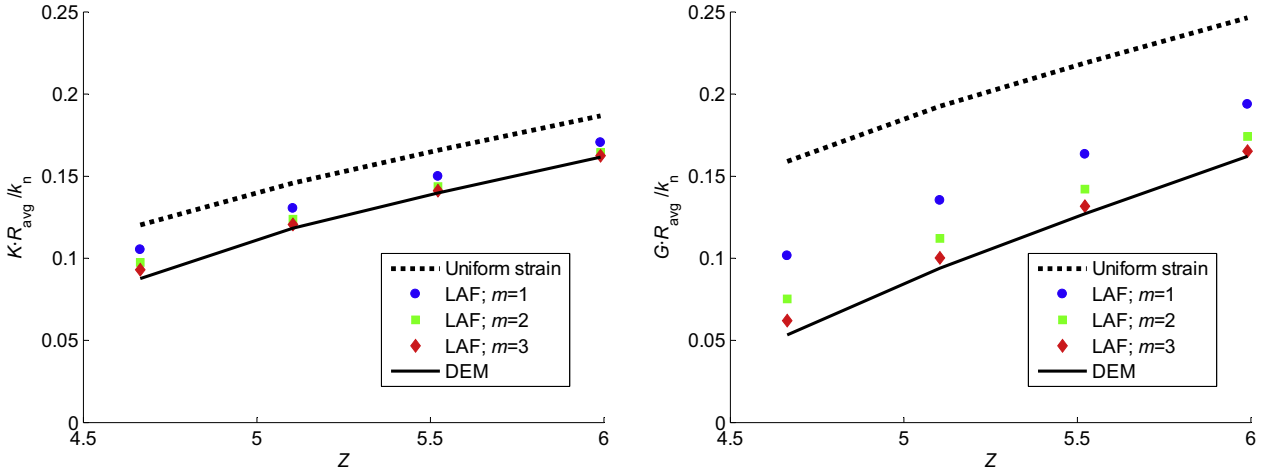

Fig. 4. Comparison of true, elastic moduli from the DEM simulations with the local-adjustment-field (LAF) approach for various assemblies with different coordination number Z and for various shell sizes m. Left: bulk modulus K; right: shear modulus G (right). Stiffness ratio $k_t/k_n = 0.8$.

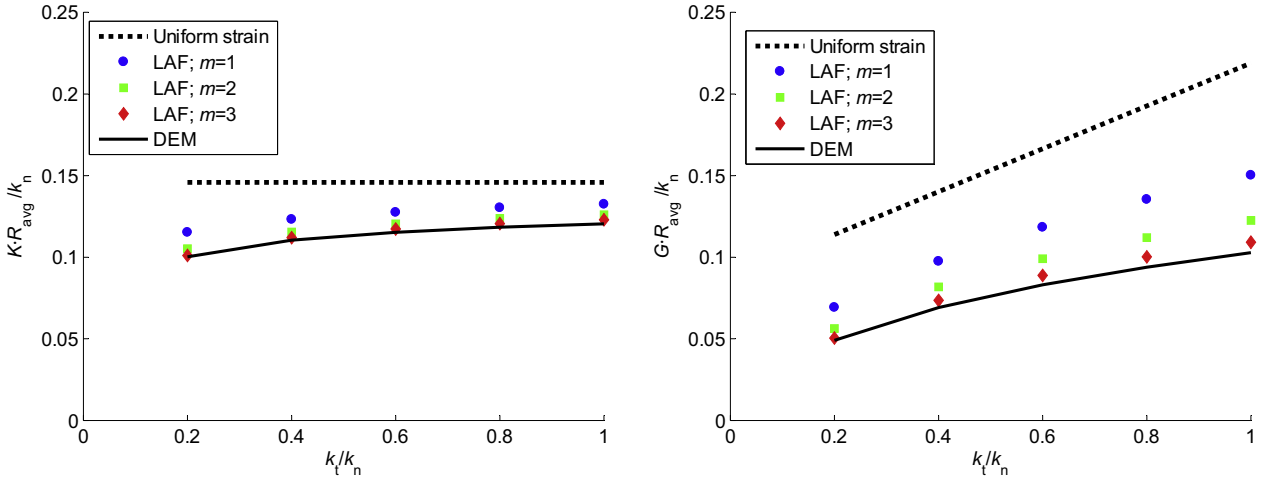

Fig. 5. Comparison of true, elastic moduli from the DEM simulations with approximations with the local-adjustment-field LAF-method for various values of the stiffness ratio k_t/k_n and for various shell sizes m. Left: bulk modulus K; right: shear modulus G. Assembly with coordination number $Z = 5.52$.

case. These rotational degrees of freedom may exhibit strong fluctuations.

For a proper comparison of these cases, assemblies with equivalent coordination numbers should be considered. For this equivalence the criterion of equal "redundancy indices" is proposed here. The redundancy index RI (Kruyt, 2010) is the ratio between the number of force degrees of freedom at the contacts over the number of equilibrium equations for the particles. Note that for a statically-determinate system without redundancy, $RI = 1$. Considering elastic contacts, the number of force degrees of freedom at contacts is $2N_c$ and $3N_c$ in the two-dimensional and three-dimensional case, respectively. The number of force and moment equilibrium equations for the particles is $3N_p$ and $6N_p$ in the two-dimensional and three-dimensional case, respectively. It follows, using $Z = (2N_c)/N_p$, that $RI_{2D} = Z/3$ and $RI_{3D} = Z/4$. The criterion of equal redundancy indices then yields that the coordination number of a two-dimensional assembly $Z_{eq,2D}$ that is equivalent to a three-dimensional assembly with coordination number Z is given by $Z_{eq,2D} = (3/4)Z$.

The current results shown in Fig. 3 for coordination number $Z = 5.52$ and stiffness ratio $k_t/k_n = 0.8$ are used as data for the three-dimensional case in the comparison. The equivalent coordination number of a two-dimensional assembly then is given by $Z_{ed,2D} = 4.14$. This value is fairly close to the coordination number of 4.08, for which data are given by Kruyt et al. (2010) (see their Fig. 7). Their stiffness ratio that is closest to the value $k_t/k_n = 0.8$ for the three-dimensional case of Fig. 3 is $k_t/k_n = 0.75$. The corresponding relative deviations between true shear modulus G and that based on the local-adjustment-field approach are, for various shell sizes m, as follows. For $m = 1$: 23% (2D), 29% (3D); for $m = 2$: 16% (2D), 12% (3D); for $m = 3$: 11% (2D), 4% (3D). This tentative comparison (considering the inexact match in coordination number and stiffness ratio) indicates that the local-adjustment-field method is at least as effective in giving accurate predictions of the moduli in the three-dimensional case as it is in the two-dimensional case.

7. Discussion

The local-adjustment-field approach for the prediction of the elastic moduli of three-dimensional isotropic granular assemblies has been proposed. In this approach the particle displacements and rotations are estimated from solutions of the equilibrium equations for small subassemblies. By increasing the size of the subassemblies, the accuracy of the predictions is improved.

Two methods are described for the evaluation of the moduli from the particle displacement and rotation fields, the stress-based

and the energy-based methods. The energy-based method provides a rigorous upper bound to the moduli, as follows from the minimum potential-energy principle. Generally, the stress-based method gives predictions of the moduli that are closer to the true elastic moduli as determined from the results of DEM simulations.

The accuracy of the predictions of bulk and shear moduli according to the local-adjustment field approach is not very sensitive to the value of the stiffness ratio k_t/k_n. Looser assemblies with lower coordination numbers Z are less constrained, and hence will show larger fluctuations in displacements and rotations. Therefore, the accuracy of the predictions of the moduli according to the local-adjustment-field approach is lower for assemblies with lower coordination numbers.

For a shell size $m = 3$ the bulk and shear moduli are well predicted (with a relative deviation that is smaller than 7%, except for the shear modulus of the loosest assembly) for the coordination numbers and stiffness ratios considered here. This corresponds to a size of the meso-scale of three particle diameters. For the assembly with the lowest coordination number ($Z = 4$) such a meso-scale involves about 20 inner particles. The size of the meso-scale is important for general, detailed micromechanical modelling of granular materials (for example Nicot and Darve, 2011).

In the current approach very detailed information on the contacts of the individual particles is employed to solve for the particle displacements and rotations from the equilibrium equations for the subassemblies. Future work will deal with analytical formulations of the current approach, in which this detailed information is replaced by suitable assumptions on statistical characteristics of the contact network.

References

Agnolin, I., Jenkins, J.T., La Ragione, L., 2006. A continuum theory for a random array of identical, elastic, frictional disks. Mech. Mater. 38, 687–701.

Agnolin, I., Roux, J.N., 2007a. Internal states of model isotropic granular packings. I. Assembling process, geometry, and contact networks. Phys. Rev. E 76, 061302.

Agnolin, I., Roux, J.N., 2007b. Internal states of model isotropic granular packings. III. Elastic properties. Phys. Rev. E 76, 061304.

Agnolin, I., Kruyt, N.P., 2008. On the elastic moduli of two-dimensional assemblies of disks: relevance and modelling of fluctuations in particle displacements and rotations. Comput. Math. Appl. 55, 245–256.

Agnolin, I., Roux, J.N., 2008. On the elastic moduli of three-dimensional assemblies of spheres: characterization and modelling of fluctuations in the particle displacement and rotation. Int. J. Solids Struct. 45, 1101–1123.

Aris, R., 1962. Vectors, Tensors, and the Basic Equations of Fluid Mechanics. Dover Publications, New York, NY, USA.

Bathurst, R.J., Rothenburg, L., 1988a. Micromechanical aspects of isotropic granular assemblies with linear contact interactions. J. Appl. Mech. (Trans. ASME) 55, 17–23.

Bathurst, R.J., Rothenburg, L., 1988b. Note on a random isotropic granular material with negative Poisson's ratio. Int. J. Eng. Sci. 26, 373–383.

Calvetti, F., Tamagnini, C., Viggiani, G., 2002. On the incremental behaviour of granular soils. In: Pande, G., Pietruszczak, S. (Eds.), Proceedings NUMOG VIII. Swets and Zeitlinger Lisse, The Netherlands, pp. 3–9.

Cambou, B., Dubujet, P., Emeriault, F., Sidoroff, F., 1995. Homogenisation for granular materials. Eur. J. Mech. A/Solids 14, 255–276.

Chang, C.S., Misra, A., 1989. Theoretical and experimental study of regular packings of granules. J. Eng. Mech. (Trans. ASCE) 115, 704–720.

Chang, C.S., Misra, A., Sundaram, S.S., 1990. Micromechanical modelling of cemented sands under low amplitude oscillations. Géotechnique 40, 251–263.

Chang, C.S., Liao, C.L., 1994. Estimates of elastic modulus for media of randomly packed granules. Appl. Mech. Rev. 47, S197–S206.

Chantawarangul, K., 1993. Numerical simulations of three-dimensional granular assemblies (Ph.D. thesis). Department of Civil Engineering, University of Waterloo, Waterloo, Ontario, Canada.

Cundall, P.A., Strack, O.D.L., 1979. A discrete numerical model for granular assemblies. Géotechnique 9, 47–65.

Deresiewicz, H., 1958. Stress–strain relations for a simple model of a granular medium. J. Appl. Mech. (Trans. ASME) 25, 402–406.

Digby, P.J., 1981. The effective moduli of porous granular rock. J. Appl. Mech. (Trans. ASME) 48, 803–808.

Fleischmann, J.A., Drugan, W.J., Plesha, M.E., 2013a. Direct micromechanics derivation and DEM confirmation of the elastic moduli of isotropic particulate materials: Part I No particle rotation. J. Mech. Phys. Solids 61, 1569–1584.

Fleischmann, J.A., Drugan, W.J., Plesha, M.E., 2013b. Direct micromechanics derivation and DEM confirmation of the elastic moduli of isotropic particulate materials: Part II Particle rotation. J. Mech. Phys. Solids 61, 1585–1599.

Goddard, J.D., 1990. Nonlinear elasticity and pressure-dependent wave speeds in granular media. Proc. R. Soc. London A 430, 105–131.

Golub, G.H., van Loan, C.F., 1996. Matrix Computations. The Johns Hopkins University Press, Baltimore, USA.

Hill, R., 1950. The Mathematical Theory of Plasticity. Clarendon Press, Oxford, UK.

Horne, M.R., 1965. The behaviour of an assembly of rotund, rigid, cohesionless particles, I and II. Proc. R. Soc. London A 286, 62–97.

Jenkins, J.T., Johnson, D., La Ragione, L., Makse, H.A., 2005. Fluctuations and the effective moduli of an isotropic, random aggregate of identical, frictionless spheres. J. Mech. Phys. Solids 53, 197–225.

Johnson, K.L., 1985. Contact Mechanics. Cambridge University Press, Cambridge, UK.

Kruyt, N.P., Rothenburg, L., 1996. Micromechanical definition of the strain tensor for granular materials. J. Appl. Mech. (Trans. ASME) 63, 706–711.

Kruyt, N.P., Rothenburg, L., 1998. Statistical theories for the elastic moduli of two-dimensional assemblies of granular materials. Int. J. Eng. Sci. 36, 1127–1142.

Kruyt, N.P., Rothenburg, L., 2002. Micromechanical bounds for the elastic moduli of granular materials. Int. J. Solids Struct. 39, 311–324.

Kruyt, N.P., Rothenburg, L., 2004. Kinematic and static assumptions for homogenization in micromechanics of granular materials. Mech. Mater. 36, 1157–1173.

Kruyt, N.P., 2010. Micromechanical study of plasticity of granular materials. Comptes Rendus Mécanique 338, 596–603.

Kruyt, N.P., Agnolin, I., Luding, S., Rothenburg, L., 2010. Micromechanical study of elastic moduli of loose granular materials. J. Mech. Phys. Solids 58, 1286–1301.

Kruyt, N.P., 2012. Micromechanical study of dispersion and damping characteristics of granular materials. J. Mech. Mater. Struct. 7, 347–361.

La Ragione, L., Jenkins, J.T., 2007. The initial response of an idealized granular material. Proc. R. Soc. London A 463, 735–758.

Magnanimo, V., La Ragione, L., Jenkins, J.T., Wang, P., Makse, H.A., 2008. Characterizing the shear and bulk moduli of an idealized granular material. EPL 81, 34006.

Makse, H.A., Gland, N., Johnson, D.L., Schwartz, L.M., 1999. Why effective medium theory fails in granular materials. Phys. Rev. Lett. 83, 5070–5073.

Makse, H.A., Gland, N., Johnson, D.L., Schwartz, L.M., 2004. Granular packings: nonlinear elasticity, sound propagation, and collective relaxation dynamics. Phys. Rev. E 70, 061302.

Nicot, F., Darve, F., 2011. The H-microdirectional model: accounting for a mesoscopic scale. Mech. Mater. 43, 918–929.

Rothenburg, L., 1980. Micromechanics of idealised granular materials (Ph.D. thesis). Department of Civil Engineering, Carleton University, Ottawa, Ontario, Canada.

Rothenburg, L., Kruyt, N.P., 2001. On limitations of the uniform strain assumption in micromechanics of granular materials. In: Kishino, Y. (Ed.), Powders & Grains 2001: 4th International Conference on Micromechanics of Granular Media. Balkema Publishers, Lisse, The Netherlands, pp. 191–194.

Tatsuoka, F., 1999. Small strain behaviour of granular materials. In: Oda, M., Iwashita, K. (Eds.), Mechanics of Granular Materials: An Introduction. Balkema Publishers, Rotterdam, The Netherlands, pp. 299–308.

Walton, K., 1987. The effective elastic moduli of a random packing of spheres. J. Mech. Phys. Solids 35, 213–226.

Wang, Y., Mora, P., 2009. Macroscopic elastic properties of regular lattices. J. Mech. Phys. Solids 56, 3456–3474.

Washizu, K., 1968. Variational Methods in Elasticity and Plasticity. Pergamon Press, Oxford, UK.